The Astrophysical Journal Letters, 926:L12 (8pp), 2022 February 20 https://doi.org/10.3847/2041-8213/ac51d8

CWISE J014611.20–050850.0AB: The Widest Known Brown Dwarf Binary in the Field

Emma Softich[1], Adam C. Schneider[2,3], Jennifer Patience[1], Adam J. Burgasser[4], Evgenya Shkolnik[1], Jacqueline K. Faherty[5], Dan Caselden[5], Aaron M. Meisner[6], J. Davy Kirkpatrick[7], Marc J. Kuchner[8], Jonathan Gagné[9,10], Daniella Bardalez Gagliuffi[5], Michael C. Cushing[11], Sarah L. Casewell[12], Christian Aganze[4], Chih-Chun Hsu[4], Nikolaj Stevnbak Andersen[13], Frank Kiwy[13], and Melina Thévenot[13]
The Backyard Worlds: Planet 9 Collaboration

[1] School of Earth and Space Exploration, Arizona State University, Tempe, AZ 85282, USA
[2] United States Naval Observatory, Flagstaff Station, 10391 West Naval Observatory Road, Flagstaff, AZ 86005, USA
[3] Department of Physics and Astronomy, George Mason University, MS3F3, 4400 University Drive, Fairfax, VA 22030, USA
[4] Center for Astrophysics and Space Science, University of California San Diego, La Jolla, CA 92093, USA
[5] Department of Astrophysics, American Museum of Natural History, Central Park West at 79th Street, New York, NY 10024, USA
[6] NSF's National Optical-Infrared Astronomy Research Laboratory, 950 North Cherry Avenue, Tucson, AZ 85719, USA
[7] IPAC, Mail Code 100-22, Caltech, 1200 East California Boulevard, Pasadena, CA 91125, USA
[8] Exoplanets and Stellar Astrophysics Laboratory, NASA Goddard Space Flight Center, 8800 Greenbelt Road, Greenbelt, MD 20771, USA
[9] Planétarium Rio Tinto Alcan, Espace pour la Vie, 4801 ave. Pierre-de Coubertin, Montréal, QC H1V 3V4, Canada
[10] Institute for Research on Exoplanets, Université de Montréal, 2900 Boulevard Édouard-Montpetit Montréal, QC H3T 1J4, Canada
[11] Ritter Astrophysical Research Center, Department of Physics and Astronomy, University of Toledo, 2801 West Bancroft Street, Toledo, OH 43606, USA
[12] Department of Physics and Astronomy, University of Leicester, University Road, Leicester LE1 7RH, UK
[13] Backyard Worlds: Planet 9, USA
Received 2022 January 3; revised 2022 January 31; accepted 2022 February 3; published 2022 February 17

Abstract

While stars are often found in binary systems, brown dwarf binaries are much rarer. Brown dwarf–brown dwarf pairs are typically difficult to resolve because they often have very small separations. Using brown dwarfs discovered with data from the Wide-field Infrared Survey Explorer (WISE) via the Backyard Worlds: Planet 9 citizen science project, we inspected other, higher-resolution, sky surveys for overlooked cold companions. During this process, we discovered the brown dwarf binary system CWISE J0146−0508AB, which we find has a very small chance alignment probability based on the similar proper motions of the components of the system. Using follow-up near-infrared spectroscopy with Keck/NIRES, we determined component spectral types of L4 and L8 (blue), making CWISE J0146−0508AB one of only a few benchmark systems with a blue L dwarf. At an estimated distance of ∼40 pc, CWISE J0146−0508AB has a projected separation of ∼129 au, making it the widest-separation brown dwarf pair found to date. We find that such a wide separation for a brown dwarf binary may imply formation in a low-density star-forming region.

Unified Astronomy Thesaurus concepts: Brown dwarfs (185); L dwarfs (894)

1. Introduction

Several of the first brown dwarf discoveries were part of binary systems with a stellar component, such as GD 165 B (Becklin & Zuckerman 1988) and Gl 229B (Nakajima et al. 1995). The first brown dwarf binary systems, defined here as systems where both components are below the hydrogen-burning minimum mass (∼0.07 $M_{\odot}$; Saumon & Marley 2008), required the use of high-resolution imaging (e.g., Martín et al. 1998; Martin et al. 1999) or high-resolution spectroscopic monitoring (e.g., Basri & Martín 1999). As with the binary fraction for stars, the brown dwarf binary fraction can help to put constraints on substellar formation theories (e.g., Bate 2009). The stellar multiplicity fraction decreases significantly with decreasing primary mass, from ∼69% for A-type stars (De Rosa et al. 2014) to ∼25%–30% for M-type stars (Ward-Duong et al. 2015; Winters et al. 2019). This decreasing binary fraction continues across the stellar–substellar boundary, with measured brown dwarf binary fractions typically between ∼10% and 20% (e.g., Burgasser et al. 2006b; Radigan et al. 2013; Aberasturi et al. 2014; Fontanive et al. 2018). Further, the semimajor axis distribution decreases significantly for substellar objects, with brown dwarf–brown dwarf separations typically of a few au (e.g., Artigau et al. 2011; Faherty et al. 2020).

There are ∼50 resolved, field-age brown dwarf binaries (Bardalez Gagliuffi et al. 2015; Faherty et al. 2020), and their median separation is ≈4 au. Only four systems have separations wider than 20 au (one of which is a hierarchical triple; Radigan et al. 2013), with the widest system known to date being SDSS J1416+1348AB (Burgasser et al. 2010b; Burningham et al. 2010; Scholz 2010), with a projected separation of ∼89 au. There are several known brown dwarf pairs with wider separations at very young ages (e.g., Chauvin et al. 2004; Luhman 2004; Close et al. 2007; Béjar et al. 2008; Luhman et al. 2009; Strampelli et al. 2020; De Furio et al. 2021), though some of these systems may still be disrupted, depending on the density of their birth environment. Note that some very wide L+L and L+T binaries exist (e.g., Faherty et al. 2020; Marocco et al. 2020), but in these cases, the L-type component is most likely stellar.

Brown dwarf binaries are most commonly found through either spectral decomposition (e.g., Burgasser et al. 2010a; Geißler et al. 2011; Bardalez Gagliuffi et al. 2014; Marocco et al. 2015) or high-resolution imaging (e.g., Reid et al. 2001; Bouy et al. 2003; Burgasser et al. 2003; Gizis et al. 2003; Burgasser et al. 2006b; Liu et al. 2006; Reid et al. 2006; Dupuy & Liu 2012; Aberasturi et al. 2014; Bardalez Gagliuffi et al. 2015; Opitz et al. 2016), with a small number of low-mass systems found through radial velocity (e.g., Basri & Martín 1999; Blake et al. 2008) or astrometric (e.g., Sahlmann et al. 2013) monitoring. Until now, only one field brown dwarf binary has been discovered as a resolved pair in wide-field survey images: the previously mentioned SDSS J1416 +1348AB, which was resolved in UKIDSS images (Burgasser et al. 2010b; Burningham et al. 2010; Scholz 2010).

In this paper, we present the discovery of the wide brown dwarf binary CWISE J014611.20−050850.0AB. We describe its discovery in Section 2 and our follow-up spectroscopic observations in Section 3. We present our analysis and discussion of the system in Sections 4 and 5.

2. Discovery

The Backyard Worlds: Planet 9 (BYW) citizen science project is a collaborative effort between professional astronomers and citizen scientists from around the world (Kuchner et al. 2017). One of the main goals of the project is to create a more complete census of substellar members of the solar neighborhood. The BYW project has so far made numerous contributions to the census of solar neighborhood members (e.g., Bardalez Gagliuffi et al. 2020; Meisner et al. 2020; Kirkpatrick et al. 2021; Schneider et al. 2021). The project has also been adept at discovering cold companions to nearby stars (e.g., Faherty et al. 2020; Faherty et al. 2021; Jalowiczor et al. 2021; Rothermich et al. 2021).

The BYW project uses data from the Wide-field Infrared Survey Explorer (WISE; Wright et al. 2010) to identify brown dwarf candidates. In an effort to identify previously unknown brown dwarf binaries, we have examined each brown dwarf candidate found through the BYW project for evidence of binarity in existing imaging surveys with higher resolution than WISE. These surveys include Pan-STARRS1 (Chambers et al. 2016), the VISTA Hemisphere Survey (VHS; McMahon et al. 2013), the UKIRT Hemisphere Survey (UHS; Dye et al. 2018), and the Dark Energy Survey (DES; the Dark Energy Survey Collaboration 2005). This search of over 3000 brown dwarf candidates returned ∼10 candidate binaries based on proximity, available colors, and proper motions. We have obtained follow-up spectroscopy for both components of one of the most promising binary candidates, CWISE J014611.20−050850.0A and CWISE J014611.20−050850.0B (hereafter CWISE J0146 −0508AB; Marocco et al. 2020), which was prioritized for follow-up observations because it had clear detections in multiple surveys (Figure 1). The remaining brown dwarf candidates will need similar follow-up observations to confirm their binary status.

Based on its significant proper motion, CWISE J0146 −0508A was submitted as an object of interest by citizen scientists Nikolaj Stevnbak, Sam Goodman, Melina Thévenot, Dan Caselden, and Frank Kiwy. The inspection of archival images of CWISE J0146−0508A from Pan-STARRS1, VHS, and DES revealed a possible resolved companion at a separation of ∼3″ (Figure 1). While the CatWISE 2020 catalog has an entry at the position of the putative secondary, the measured proper motions from the CatWISE 2020 catalog are significantly different than CWISE J0146−0508A, likely due to the sources being blended in the WISE images. The positions and photometry from each survey for both components of the pair are listed in Table 1.

3. Observations

3.1. Keck/NIRES

To measure the spectral types of CWISE J0146−0508A and CWISE J0146−0508B, we observed both components with the Near-Infrared Echellette Spectrometer (NIRES; Wilson et al. 2004) located on the Keck II telescope on UT 2020 October 22. NIRES provides $R \sim 2700$ spectra from 0.9 to 2.45 μm. For each component, eight 300 s exposures were taken for total on-source integration times of 2400 s. Each target was nodded along the slit in an ABBA pattern. The A0 star HD 216807 was observed for telluric correction purposes. The spectra were extracted using a modified version of the SpeXTool package (Vacca et al. 2003; Cushing et al. 2004). We achieved a signal-to-noise ratio (S/N) of 400 and 1000 for the J and K peaks of the A component, respectively, and 50 and 200 for the J and K peaks of the B component. The final reduced spectra are shown in Figure 2.

4. Analysis

4.1. Spectral Types

Spectral types for each component were determined by comparing *J*-band morphologies to near-infrared spectral standards from Burgasser et al. (2006a) and Kirkpatrick et al. (2010). We found a best-fit type of L4 ± 0.5 subtypes for the A component and L8 ± 0.5 subtypes for the B component (Figure 2). CWISE J0146−0508B appears bluer than the L8 spectral standard, and we therefore give it a spectral type designation of L8 (blue). Neither spectrum shows signs of being a spectral binary according to the spectral indices of Bardalez Gagliuffi et al. (2014, 2015).

4.2. Proper Motion and Chance Alignment Probability

Though CWISE J0146−0508A has an entry in the Gaia EDR3 catalog (Gaia Collaboration et al. 2021), it includes no measured proper-motion or parallax values. This is likely because CWISE J0146−0508A has a Gaia *G* magnitude of 20.99, which is fainter than the nominal $G = 20.7$ mag survey limit.

Even though CWISE J0146−0508A and CWISE J0146 −0508B are resolved in the CatWISE 2020 catalog, they are blended in WISE images (Figure 1), making their CatWISE measured proper motions potentially unreliable. For this reason, we calculated the proper motion of each component using the available astrometric measurements for which this pair is well resolved. We used the single-epoch positions of each component from the NOIRLab Source Catalog (NSC) DR2 (Nidever et al. 2021) and Pan-STARRS1 DR2 (Flewelling 2018). The NSC contains single-epoch measurements from the Dark Energy Camera (DECam) on the CTIO 4 m. For CWISE J0146−0508A, there are 31 single-epoch NSC DR2 detections and 55 single-epoch Pan-STARRS1 DR2 detections. For CWISE J0146−0508B, there are 22 single-epoch NSC DR2 detections and nine single-epoch Pan-STARRS1 DR2

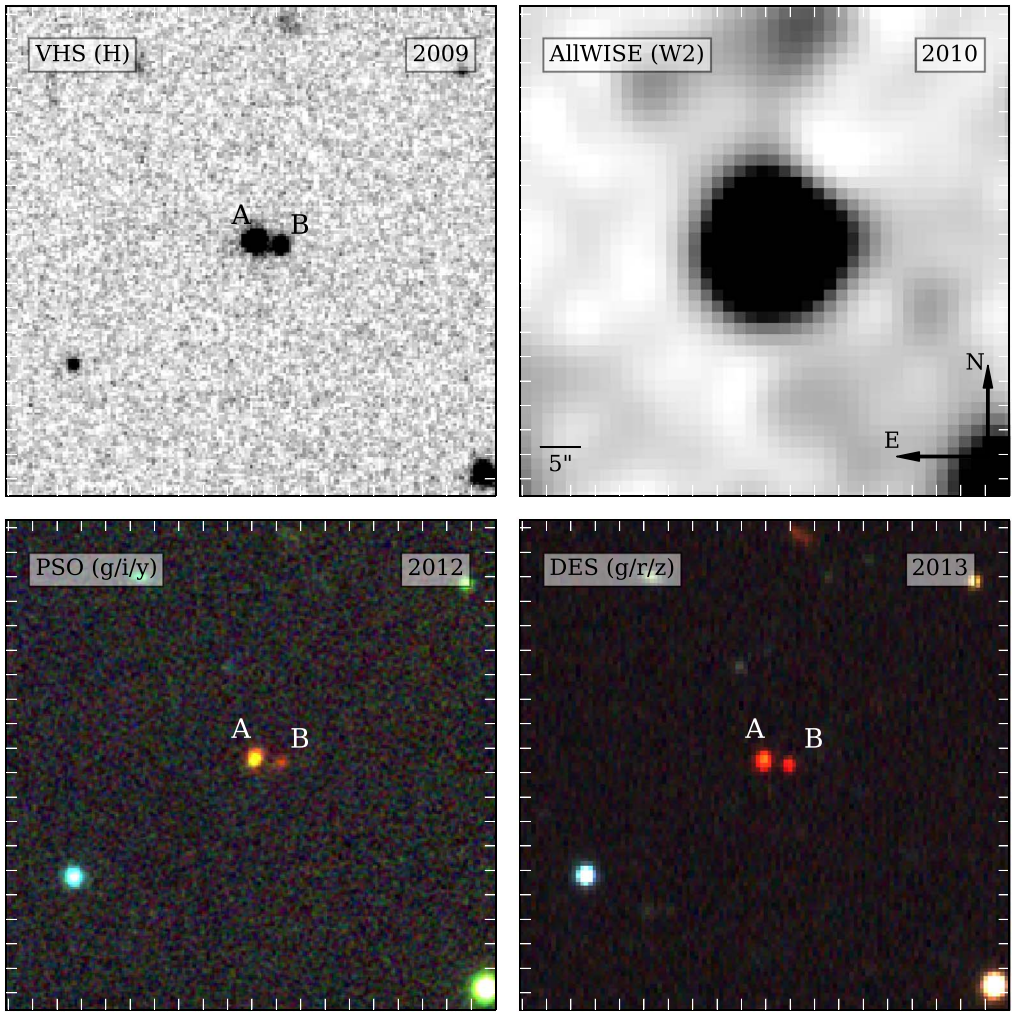

Figure 1. Survey images of CWISE J0146−0508AB. From top left to bottom right: VHS (H), AllWISE (W2), Pan-STARRS1 three-color ($g/i/y$), and DES three-color ($g/r/z$). While it is difficult to resolve CWISE J0146−0508AB in the AllWISE image, it is clearly resolved as a double in the VHS, Pan-STARRS, and DES images. Note also that the reddish color of each component in the Pan-STARRS1 and DES images indicates very red optical colors, typical of cold brown dwarfs. Each image is $1' \times 1'$.

detections. For both objects, these positional measurements span a range of just over 9 yr, from 2009 to 2018. There are significantly fewer Pan-STARRS1 DR2 detections of CWISE J0146−0508B than CWISE J0146−0508A because CWISE J0146−0508B was not detected with the i-band filter in any epoch (CWISE J0146−0508A has 19 i-band detections) and is near the 5σ Pan-STARRS1 single-epoch detection limits of 20.9 mag at the z band and 19.7 mag at the y band (Chambers et al. 2016).

We calculated proper motions using a least-squares fit weighted by the quoted uncertainty of each astrometric measurement. For CWISE J0146−0508A, we find $\mu_\alpha = 79.14 \pm 1.10$ and $\mu_\delta = -214.40 \pm 1.03$ mas yr^{-1}. For CWISE J0146−0508B, we find $\mu_\alpha = 83.94 \pm 3.43$ and $\mu_\delta = -210.33 \pm 3.35$ mas yr^{-1}. These values are fully consistent with the proper-motion values given in the NSC DR2 for CWISE J0146−0508A ($\mu_\alpha = 81.79 \pm 1.98$ and $\mu_\delta = -218.51 \pm 1.93$ mas yr^{-1}) and CWISE J0146−0508B ($\mu_\alpha = 80.52 \pm 4.85$ and $\mu_\delta = -214.01 \pm 4.75$ mas yr^{-1}).

The small separation of this pair ($\sim 3''$) and the similarity of their proper-motion components (within $\sim 1\sigma$) suggests that this is likely a physical pair. We use the `CoMover` code (Gagné et al. 2021; Schneider et al. 2021) to evaluate the possibility that this pair is the result of a chance alignment. We find a >99% probability that this is a physically associated pair.

4.3. Distance/Separation

Kirkpatrick et al. (2021) provided relations between absolute magnitude and spectral type for L-, T-, and Y-type brown dwarfs within 20 pc. Using their relations for J and H, we find a distance of 41.5 ± 2.5 pc for CWISE J0146−0508A and 40.0 ± 3.0 pc for CWISE J0146−0508B using weighted averages for J and H. We give a conservative estimate for the distance of the pair of 41 ± 5 pc.

The average separation between CWISE J0146−0508A and CWISE J0146−0508B from NSC DR2 and Pan-STARRS1 DR2 measurements is $3\farcs14 \pm 0\farcs8$. Using our distance estimate and measured separation, we find a projected separation of 129 ± 15 au for this pair. We account for inclination angle and eccentricity effects when converting to a physical separation following Dupuy & Liu (2011) and find a separation of 149^{+104}_{-41} au.

Table 1
Properties of CWISE J0146−0508AB Components

Parameter	CWISE J0146−0508A	CWISE J0146−0508B
This Work		
μ_α (mas yr^{-1})	79.14 ± 1.10	83.94 ± 3.43
μ_δ (mas yr^{-1})	-214.40 ± 1.03	-210.33 ± 3.35
Spec. type	L4	L8 (blue)
$T_{\rm eff}$ (K)	1720 ± 150	1340 ± 140
Mass ($M_{\rm Jup}$)[a]	72 ± 6	66 ± 10
CatWISE 2020		
R.A. (J2000) (deg)	26.5467046	26.5458109
decl. (J2000) (deg)	−5.1472375	−5.1473468
W1 (mag)	13.779 ± 0.028	15.069 ± 0.027
W2 (mag)	13.507 ± 0.029	14.753 ± 0.029
Pan-STARRS1 DR2		
R.A. (J2000) (deg)	26.54666153	26.54576435
decl. (J2000) (deg)	−5.14708987	−5.1472229
i (mag)	20.692 ± 0.020	...
z (mag)	19.125 ± 0.019	20.476 ± 0.032
y (mag)	18.074 ± 0.012	19.379 ± 0.124
DES DR1		
R.A. (J2000) (deg)	26.546694	26.545828
decl. (J2000) (deg)	−5.147201	−5.147353
i (mag)	20.136 ± 0.011	22.089 ± 0.061
z (mag)	18.588 ± 0.006	20.055 ± 0.020
Y (mag)	18.057 ± 0.008	19.572 ± 0.028
VHS DR6		
R.A. (J2000) (deg)	26.5465517	26.5456781
decl. (J2000) (deg)	−5.1469086	−5.147062
J (mag)	15.818 ± 0.005	17.420 ± 0.018
H (mag)	15.044 ± 0.006	16.524 ± 0.019
K_S (mag)	14.347 ± 0.006	15.790 ± 0.021

Note.
[a] Estimated using the Phillips et al. (2020) evolutionary models.

4.4. Physical Properties (Effective Temperature, Age, and Mass)

Using our derived spectral types and a spectral type uncertainty of ±0.5 subtypes, we find effective temperature ($T_{\rm eff}$) values of 1720 ± 150 and 1340 ± 140 K for CWISE J0146−0508A and CWISE J0146−0508B, respectively, using the spectral type versus $T_{\rm eff}$ relation from Kirkpatrick et al. (2021).

Neither CWISE J0146−0508A nor CWISE J0146−0508B show any signs of youth in their spectra, as a low surface gravity will typically show weakened absorption features from FeH and alkali lines and stronger absorption from VO (Allers & Liu 2013). We find a gravity classification of FLD-G for CWISE J0146−0508A using the classification scheme of Allers & Liu (2013). The Allers & Liu (2013) gravity classification method does not extend to L8 spectral types, so is not applicable to CWISE J0146−0508B. We note that most young, late L-type brown dwarfs are significantly redder than field-age standards (e.g., Gizis et al. 2012; Faherty et al. 2013; Liu et al. 2013; Schneider et al. 2014; Kellogg et al. 2016; Schneider et al. 2016). On the other hand, CWISE J0146−0508B is bluer than the L8 standard (Figure 2). This is also seen in the measured $J-K$ color of CWISE J0146−0508B (1.63 mag), which is on the blue end of the field-age L8 $J-K$ color distribution ($\sim 1.78 \pm 0.16$ mag; Faherty et al. 2016). A blue color is generally attributed to thin condensate clouds and/or old age (e.g., Cushing et al. 2010; Burgasser et al. 2010b) or perhaps viewing geometry (Vos et al. 2017). Therefore, CWISE J0146−0508B is a compelling benchmark target for clarifying the nature of the blue L dwarf population. These characteristics imply that the CWISE J0146−0508AB system is not young.

While a blue near-infrared color is a trait common to low-metallicity, old ($\gtrsim$10 Gyr) subdwarfs, CWISE J0146−0508B is not nearly as blue as the sdL7 standard from Greco et al. (2019). Brown dwarfs with spectral types of sdL7 or sdL8 in Zhang et al. (2018) have $J-K$ colors between 0.9 and 1.3 mag, much bluer than that found for CWISE J0146−0508B (1.63 mag). Further, CWISE J0146−0508A is a good match to the L4 standard at all wavelengths. Using the proper motion we derived for CWISE J0146−0508A and our estimated distance from Section 4.3, we find a tangential velocity for this system of $\sim$44 km s^{-1}, consistent with the thin disk population (e.g., Nissen 2004). We therefore conclude that CWISE J0146−0508A and CWISE J0146−0508B are not subdwarfs. We assume a conservative age range of 0.5–10 Gyr for this pair.

Using our derived $T_{\rm eff}$ values and this age range, we find a mass of 72 ± 6 $M_{\rm Jup}$ for CWISE J0146−0508A and 66 ± 10 $M_{\rm Jup}$ for CWISE J0146−0508B using the evolutionary models of Phillips et al. (2020). Uncertainties are determined in a Monte Carlo fashion using a uniform probability distribution for age over the range 0.5–10 Gyr and a normal distribution for $T_{\rm eff}$. We also calculate masses using the hybrid evolutionary models of Saumon & Marley (2008) and find fully consistent results of 74 ± 5 and 64 ± 10 $M_{\rm Jup}$ for CWISE J0146−0508A and CWISE J0146−0508B, respectively. While the current mass estimate for CWISE J0146−0508A suggests that there is a possibility that it is stellar and not a brown dwarf, previous studies of the location of the stellar/substellar boundary have found it to occur at a spectral type of ≈L4 or earlier (Dieterich et al. 2014; Dupuy & Liu 2017), making CWISE J0146−0508A most likely substellar in nature. More precise mass estimates for each component will require a tighter age constraint.

5. Discussion

5.1. Binding Energy

Using the estimated separation (149^{+104}_{-41} au) and the masses of CWISE J0146−0508A (72 ± 6 $M_{\rm Jup}$) and CWISE J0146−0508B (66 ± 10 $M_{\rm Jup}$), we calculate the binding energy of this system. We find a binding energy of $4.0^{+0.9}_{-0.7} \times 10^{41}$ erg. This is one of the lowest binding energies found for field-age brown dwarf–brown dwarf pairs (Faherty et al. 2020).

Previous investigations have found that wide brown dwarf binaries with separations greater than a few tens of au are exceptionally rare, especially at field ages. There have been several efforts to describe the largest possible separations for low-mass systems, both empirically (Reid et al. 2001; Burgasser et al. 2003; Close et al. 2003; Dhital et al. 2010) and theoretically (Zuckerman & Song 2009; Faherty et al. 2010). Specifically for brown dwarf binaries, Burgasser et al. (2003) showed that being disrupted through chance encounters with either a star or giant molecular clouds was unlikely, and thus dissipation due to random encounters could not explain the

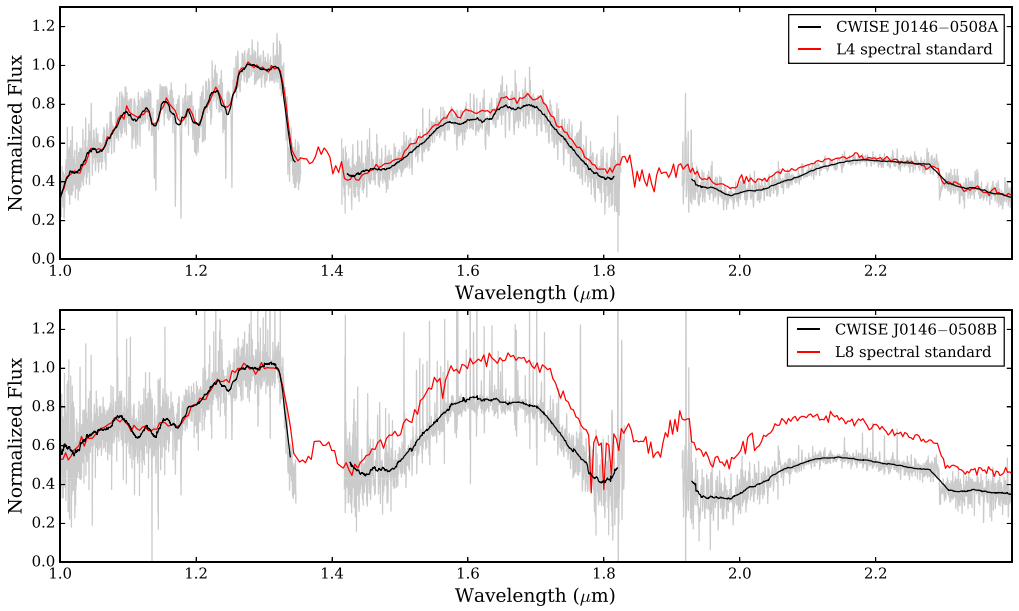

Figure 2. Keck/NIRES spectra of CWISE J0146−0508A (top) and CWISE J0146−0508B (bottom) compared to the L4 (2MASS J21580457−1550098; Kirkpatrick et al. 2010) and L8 (2MASSW J1632291+190441; Burgasser 2007) spectral standards following Kirkpatrick (2005). The spectra of CWISE J0146−0508A and CWISE J0146−0508B are shown at full resolution (gray lines) and smoothed to the resolution of the spectral standards (black lines). All spectra have been normalized between 1.27 and 1.29 μm.

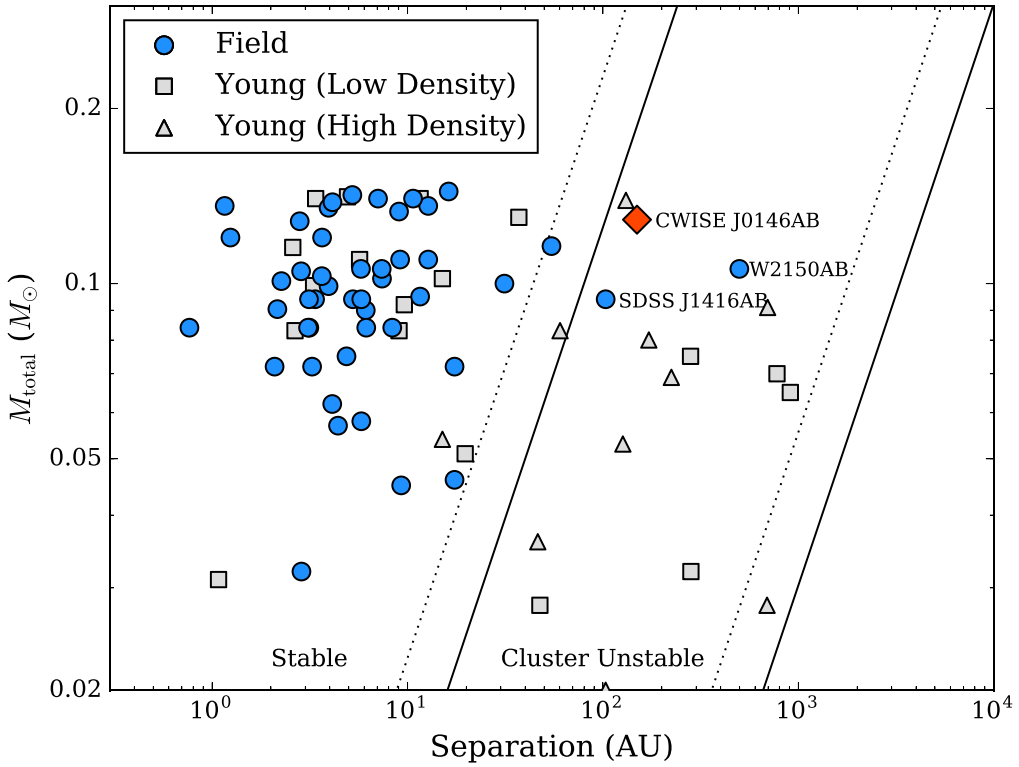

Figure 3. Separation vs. total mass for all resolved binaries from Faherty et al. (2020), Strampelli et al. (2020), and De Furio et al. (2021), where each component has a mass less than $<0.075\ M_\odot$. Field-age pairs are represented by blue circles, while young binaries from dense regions (e.g., the ONC) are shown as gray triangles and young binaries from low-density regions (e.g., Taurus, Chamaeleon, and ρ Ophiuchus) are shown as gray squares. Dotted and solid lines show the instability regions defined in Close et al. (2007), with dotted lines representing the maximum bound separations for cluster (left) and field (right) due to diffusion and solid lines representing maximum separations due to close catastrophic encounters. These regions are most relevant to the young objects in high-density star-forming regions.

lack of wide brown dwarf binaries. Close et al. (2007) performed a similar investigation considering birth environments, which they estimated to be several thousand times more dense than the typical Galactic field. Therefore, a star or brown dwarf would have a much higher probability of chance encounters in its higher-density birth environment. They found that 10 Myr in a dense cluster environment would be much more disruptive for a binary brown dwarf than 10 Gyr in the field. They suggested that the known young ($\lesssim$10 Myr) wide ($\gtrsim$20 au) brown dwarf binaries are therefore in the process of

being disrupted. This would explain why wide brown dwarf binaries have been found in young clusters, but very few have been found at field ages. However, we note here that the cluster density used by Close et al. (2007), $n_* \sim 1000\,\mathrm{pc}^{-3}$, is likely an underestimate for the densest star-forming regions, like the Orion Nebula Cluster (ONC, $n_* \sim 3700\,\mathrm{pc}^{-3}$; De Furio et al. 2021), and a significant overestimate for low-density regions such as Taurus ($n_* \sim 1$–$10\,\mathrm{pc}^{-3}$; Luhman 2018). This is further complicated by the fact that cluster densities change as the cluster ages (e.g., Parker 2014).

Figure 3 shows the projected separations and total masses for all resolved binaries from Faherty et al. (2020), with each component having a mass near the substellar boundary (<0.075 $M_\odot$; Saumon & Marley 2008). All projected separations from Faherty et al. (2020) are multiplied by 1.16 following Dupuy & Liu (2011). To this list, we add the recent substellar binaries discovered in the ONC from Strampelli et al. (2020) and De Furio et al. (2021). Close et al. (2007) defined instability regions based on gradual tidal diffusion and close catastrophic encounters for field and cluster densities. Close et al. (2007) suggested that the young brown dwarf binaries in the "Cluster Unstable" region of Figure 3 will likely dissipate before joining the field. Since the study of Close et al. (2007), there are now three field-age binaries that reside in the "Cluster Unstable" region: CWISE J0146−0508AB, SDSS J1416+1348AB (Burgasser et al. 2010b; Burningham et al. 2010; Scholz 2010), and WISE 2150−7520AB (Faherty et al. 2020). While the A component of WISE 2150−7520AB, with a spectral type of L1, is likely stellar (Dieterich et al. 2014; Dupuy & Liu 2017), it is just above the stellar/substellar boundary; thus, its survival as a system is similarly puzzling as that of CWISE J0146−0508AB and SDSS J1416+1348AB.

As discussed in Luhman (2012) and Todorov et al. (2014), while most stars and brown dwarfs likely form in high-density environments like the ONC, where wide brown dwarf binary survival is unlikely, some fraction form in lower-density regions like Taurus (Luhman et al. 2009) and Chamaeleon (Luhman 2004), where the probability of survival is much higher. It may be that systems such as CWISE J0146−0508AB, SDSS J1416+1348AB, and WISE 2150−7520AB formed in such a relatively low-density region, allowing them to have survived as low-mass binaries at such wide separations to field ages.

Resolved brown dwarf binaries are often found to be valuable as benchmarks for measuring dynamical masses from orbital monitoring (e.g., Konopacky et al. 2010; Dupuy & Liu 2017). Assuming our measured separation is the true semimajor axis of the system, and using the masses found in Section 4.4, we find an orbital period of ∼5000 yr. Therefore, the ∼9 yr of observations so far have covered less than 0.2% of an orbital period. While it has recently been shown that accurate orbital parameters can be produced with only a small fraction of the orbit having been monitored (e.g., Blunt et al. 2017), obtaining a fraction of CWISE J0146−0508AB's orbit greater than a few percent would be beyond our lifetimes.

5.2. Future Work

The vast majority of the current census of known field brown dwarfs was discovered with wide-field infrared surveys such as 2MASS or WISE. Subsequently, new higher-resolution surveys have been produced, such as the VHS, UHS, Pan-STARRS1, and DES. The process demonstrated in this paper shows the value of reexamining known or suspected brown dwarf candidates for evidence of close companions. It is possible that the examination of images from these surveys for previously missed companions to known brown dwarfs may prove similarly fruitful. By expanding this analysis to all confirmed brown dwarfs, we would be able to develop a more comprehensive census of exceptionally wide brown dwarf binary systems. Such a survey would be complementary to focused high-resolution imaging surveys (e.g., Bardalez Gagliuffi et al. 2015; Fontanive et al. 2018) and other binary identification techniques (e.g., Deacon et al. 2017) that may not be sensitive to such wide companions. Further, the future Roman Space Telescope (Spergel et al. 2015) and Euclid (Laureijs et al. 2011) space missions will have Hubble Space Telescope–like resolution in the near-infrared over large areas of the sky, allowing for brown dwarf binary surveys at much smaller separations than are currently achievable with ground-based imaging surveys.

Such binaries have the potential to be used as valuable benchmark systems for atmospheric retrievals, which can determine chemical abundances, metallicities, and temperature–pressure profiles (e.g., Line et al. 2015; Burningham et al. 2017; Line et al. 2017; Zalesky et al. 2019; Gonzales et al. 2020). Presumably, CWISE J0146−0508A and CWISE J0146−0508B formed out of the same cloud of gas and dust and should therefore have similar elemental abundances. This pair can then be used as a test for such retrieval methods. And, because CWISE J0146−0508A has a two-parameter (R.A. and decl.) solution in Gaia EDR3, we can expect a full five-parameter solution (R.A., decl., parallax, and proper-motion components) in a future Gaia release (Fabricius et al. 2021). As a benchmark system containing a blue L dwarf, CWISE J0146−0508AB may be able to elucidate the unique atmospheric chemistry of such objects and help to probe cloud properties across the L/T transition (Brock et al. 2021).

The Backyard Worlds: Planet 9 team would like to thank the many Zooniverse volunteers who have participated in this project. We would also like to thank the Zooniverse web development team for their work creating and maintaining the Zooniverse platform and the Project Builder tools. This research was supported by NASA grant 2017-ADAP17-0067. This material is based upon work supported by the National Science Foundation under grant Nos. 2007068, 2009136, and 2009177.

Some of the data presented herein were obtained at the W. M. Keck Observatory, which is operated as a scientific partnership among the California Institute of Technology, the University of California, and the National Aeronautics and Space Administration. The Observatory was made possible by the generous financial support of the W. M. Keck Foundation. This publication makes use of data products from the Wide-field Infrared Survey Explorer, which is a joint project of the University of California, Los Angeles, and the Jet Propulsion Laboratory/California Institute of Technology, and NEOWISE, which is a project of the Jet Propulsion Laboratory/California Institute of Technology. WISE and NEOWISE are funded by the National Aeronautics and Space Administration. The authors wish to recognize and acknowledge the very significant cultural role and reverence that the summit of Maunakea has always had within the indigenous Hawaiian

community. We are most fortunate to have the opportunity to conduct observations from this mountain.

The Pan-STARRS1 Surveys (PS1) and the PS1 public science archive have been made possible through contributions by the Institute for Astronomy, the University of Hawaii, the Pan-STARRS1 Project Office, the Max Planck Society and its participating institutes, the Max Planck Institute for Astronomy, Heidelberg, and the Max Planck Institute for Extraterrestrial Physics, Garching, The Johns Hopkins University, Durham University, the University of Edinburgh, the Queen's University Belfast, the Harvard-Smithsonian Center for Astrophysics, the Las Cumbres Observatory Global Telescope Network Incorporated, the National Central University of Taiwan, the Space Telescope Science Institute, the National Aeronautics and Space Administration under grant No. NNX08AR22G issued through the Planetary Science Division of the NASA Science Mission Directorate, National Science Foundation grant No. AST-1238877, the University of Maryland, Eotvos Lorand University (ELTE), Los Alamos National Laboratory, and the Gordon and Betty Moore Foundation.

Facility: Keck (NIRES).

Software: SpeXTool (Cushing et al. 2010); SPLAT (Burgasser & Splat Development Team 2017); CoMover (Gagné et al. 2021).

ORCID iDs

Emma Softich https://orcid.org/0000-0002-1420-1837
Adam C. Schneider https://orcid.org/0000-0002-6294-5937
Jennifer Patience https://orcid.org/0000-0001-9004-803X
Adam J. Burgasser https://orcid.org/0000-0002-6523-9536
Evgenya Shkolnik https://orcid.org/0000-0002-7260-5821
Jacqueline K. Faherty https://orcid.org/0000-0001-6251-0573
Dan Caselden https://orcid.org/0000-0001-7896-5791
Aaron M. Meisner https://orcid.org/0000-0002-1125-7384
J. Davy Kirkpatrick https://orcid.org/0000-0003-4269-260X
Marc J. Kuchner https://orcid.org/0000-0002-2387-5489
Jonathan Gagné https://orcid.org/0000-0002-2592-9612
Daniella Bardalez Gagliuffi https://orcid.org/0000-0001-8170-7072
Michael C. Cushing https://orcid.org/0000-0001-7780-3352
Sarah L. Casewell https://orcid.org/0000-0003-2478-0120
Christian Aganze https://orcid.org/0000-0003-2094-9128
Chih-Chun Hsu https://orcid.org/0000-0002-5370-7494
Nikolaj Stevnbak Andersen https://orcid.org/0000-0003-4714-3829
Frank Kiwy https://orcid.org/0000-0001-8662-1622
Melina Thévenot https://orcid.org/0000-0001-5284-9231

References

Aberasturi, M., Burgasser, A. J., Mora, A., et al. 2014, AJ, 148, 129
Allers, K. N., & Liu, M. C. 2013, ApJ, 772, 79
Artigau, É, Lafrenière, D., Doyon, R., et al. 2011, ApJ, 739, 48
Bardalez Gagliuffi, D. C., Gelino, C. R., & Burgasser, A. J. 2015, AJ, 150, 163
Bardalez Gagliuffi, D. C., Burgasser, A. J., Gelino, C. R., et al. 2014, ApJ, 794, 143
Bardalez Gagliuffi, D. C., Faherty, J. K., Schneider, A. C., et al. 2020, ApJ, 895, 145
Basri, G., & Martín, E. L. 1999, AJ, 118, 2460
Bate, M. R. 2009, MNRAS, 392, 590
Becklin, E. E., & Zuckerman, B. 1988, Natur, 336, 656
Béjar, V. J. S., Zapatero Osorio, M. R., Pérez-Garrido, A., et al. 2008, ApJL, 673, L185
Blake, C. H., Charbonneau, D., White, R. J., et al. 2008, ApJL, 678, L125
Blunt, S., Nielsen, E. L., De Rosa, R. J., et al. 2017, AJ, 153, 229
Bouy, H., Brandner, W., Martín, E. L., et al. 2003, AJ, 126, 1526
Brock, L., Barman, T., Konopacky, Q. M., & Stone, J. M. 2021, ApJ, 914, 124
Burgasser, A. J. 2007, ApJ, 659, 655
Burgasser, A. J., Cruz, K. L., Cushing, M., et al. 2010a, ApJ, 710, 1142
Burgasser, A. J., Geballe, T. R., Leggett, S. K., Kirkpatrick, J. D., & Golimowski, D. A. 2006a, ApJ, 637, 1067
Burgasser, A. J., Kirkpatrick, J. D., Cruz, K. L., et al. 2006b, ApJS, 166, 585
Burgasser, A. J., Kirkpatrick, J. D., Reid, I. N., et al. 2003, ApJ, 586, 512
Burgasser, A. J., Looper, D., & Rayner, J. T. 2010b, AJ, 139, 2448
Burgasser, A. J. & Splat Development Team 2017, in Astronomical Society of India Conf. Ser., 14, ed. L. Coelho et al. (Bangalore: Astronomical Society of India), 7
Burningham, B., Marley, M. S., Line, M. R., et al. 2017, MNRAS, 470, 1177
Burningham, B., Leggett, S. K., Lucas, P. W., et al. 2010, MNRAS, 404, 1952
Chambers, K. C., Magnier, E. A., Metcalfe, N., et al. 2016, arXiv:1612.05560
Chauvin, G., Lagrange, A. M., Dumas, C., et al. 2004, A&A, 425, L29
Close, L. M., Siegler, N., Freed, M., & Biller, B. 2003, ApJ, 587, 407
Close, L. M., Zuckerman, B., Song, I., et al. 2007, ApJ, 660, 1492
Cushing, M. C., Saumon, D., & Marley, M. S. 2010, AJ, 140, 1428
Cushing, M. C., Vacca, W. D., & Rayner, J. T. 2004, PASP, 116, 362
De Furio, M., Meyer, M. R., Reiter, M., et al. 2022, ApJ, 925, 112
De Rosa, R. J., Patience, J., Wilson, P. A., et al. 2014, MNRAS, 437, 1216
Deacon, N. R., Magnier, E. A., Best, W. M. J., et al. 2017, MNRAS, 468, 3499
Dhital, S., West, A. A., Stassun, K. G., & Bochanski, J. J. 2010, AJ, 139, 2566
Dieterich, S. B., Henry, T. J., Jao, W.-C., et al. 2014, AJ, 147, 94
Dupuy, T. J., & Liu, M. C. 2011, ApJ, 733, 122
Dupuy, T. J., & Liu, M. C. 2012, ApJS, 201, 19
Dupuy, T. J., & Liu, M. C. 2017, ApJS, 231, 15
Dye, S., Lawrence, A., Read, M. A., et al. 2018, MNRAS, 473, 5113
Fabricius, C., Luri, X., Arenou, F., et al. 2021, A&A, 649, A5
Faherty, J. K., Burgasser, A. J., West, A. A., et al. 2010, AJ, 139, 176
Faherty, J. K., Rice, E. L., Cruz, K. L., Mamajek, E. E., & Núñez, A. 2013, AJ, 145, 2
Faherty, J. K., Riedel, A. R., Cruz, K. L., et al. 2016, ApJS, 225, 10
Faherty, J. K., Goodman, S., Caselden, D., et al. 2020, ApJ, 889, 176
Faherty, J. K., Gagné, J., Popinchalk, M., et al. 2021, ApJ, 923, 48
Flewelling, H. 2018, AAS Meeting, 231, 436.01
Fontanive, C., Biller, B., Bonavita, M., & Allers, K. 2018, MNRAS, 479, 2702
Gagné, J., Faherty, J. K., Schneider, A. C., & Meisner, A. M. 2021, CoMover: Bayesian Probability of Co-moving Stars, Astrophysics Source Code Library, ascl:2106.007
Gaia Collaboration, Brown, A. G. A., Vallenari, A., et al. 2021, A&A, 649, A1
Geißler, K., Metchev, S., Kirkpatrick, J. D., Berriman, G. B., & Aooper, D. 2011, ApJ, 732, 56
Gizis, J. E., Reid, I. N., Knapp, G. R., et al. 2003, AJ, 125, 3302
Gizis, J. E., Faherty, J. K., Liu, M. C., et al. 2012, AJ, 144, 94
Gonzales, E. C., Burningham, B., Faherty, J. K., et al. 2020, ApJ, 905, 46
Greco, J. J., Schneider, A. C., Cushing, M. C., Kirkpatrick, J. D., & Burgasser, A. J. 2019, AJ, 158, 182
Jalowiczor, P. A., Casewell, S., Schneider, A. C., et al. 2021, RNAAS, 5, 76
Kellogg, K., Metchev, S., Gagné, J., & Faherty, J. 2016, ApJL, 821, L15
Kirkpatrick, J. D. 2005, ARA&A, 43, 195
Kirkpatrick, J. D., Looper, D. L., Burgasser, A. J., et al. 2010, ApJS, 190, 100
Kirkpatrick, J. D., Gelino, C. R., Faherty, J. K., et al. 2021, ApJS, 253, 7
Konopacky, Q. M., Ghez, A. M., Barman, T. S., et al. 2010, ApJ, 711, 1087
Kuchner, M. J., Faherty, J. K., Schneider, A. C., et al. 2017, ApJL, 841, L19
Laureijs, R., Amiaux, J., Arduini, S., et al. 2011, arXiv:1110.3193
Line, M. R., Teske, J., Burningham, B., Fortney, J. J., & Marley, M. S. 2015, ApJ, 807, 183
Line, M. R., Marley, M. S., Liu, M. C., et al. 2017, ApJ, 848, 83
Liu, M. C., Leggett, S. K., Golimowski, D. A., et al. 2006, ApJ, 647, 1393
Liu, M. C., Magnier, E. A., Deacon, N. R., et al. 2013, ApJL, 777, L20
Luhman, K. L. 2004, ApJ, 614, 398
Luhman, K. L. 2012, ARA&A, 50, 65
Luhman, K. L. 2018, AJ, 156, 271
Luhman, K. L., Mamajek, E. E., Allen, P. R., Muench, A. A., & Finkbeiner, D. P. 2009, ApJ, 691, 1265
Marocco, F., Jones, H. R. A., Day-Jones, A. C., et al. 2015, MNRAS, 449, 3651
Marocco, F., Smart, R. L., Mamajek, E. E., et al. 2020, MNRAS, 494, 4891
Martin, E. L., Brandner, W., & Basri, G. 1999, Sci, 283, 1718
Martín, E. L., Basri, G., Brandner, W., et al. 1998, ApJL, 509, L113

McMahon, R. G., Banerji, M., Gonzalez, E., et al. 2013, Msngr, 154, 35
Meisner, A. M., Faherty, J. K., Kirkpatrick, J. D., et al. 2020, ApJ, 899, 123
Nakajima, T., Oppenheimer, B. R., Kulkarni, S. R., et al. 1995, Natur, 378, 463
Nidever, D. L., Dey, A., Fasbender, K., et al. 2021, AJ, 161, 192
Nissen, P. E. 2004, in Origin and Evolution of the Elements, ed. A. McWilliam & M. Rauch (Cambridge: Cambridge Univ. Press), 154
Opitz, D., Tinney, C. G., Faherty, J. K., et al. 2016, ApJ, 819, 17
Parker, R. J. 2014, MNRAS, 445, 4037
Phillips, M. W., Tremblin, P., Baraffe, I., et al. 2020, A&A, 637, A38
Radigan, J., Jayawardhana, R., Lafrenière, D., et al. 2013, ApJ, 778, 36
Reid, I. N., Gizis, J. E., Kirkpatrick, J. D., & Koerner, D. W. 2001, AJ, 121, 489
Reid, I. N., Lewitus, E., Allen, P. R., Cruz, K. L., & Burgasser, A. J. 2006, AJ, 132, 891
Rothermich, A., Schneider, A. C., Faherty, J. K., et al. 2021, RNAAS, 5, 18
Sahlmann, J., Lazorenko, P. F., Ségransan, D., et al. 2013, A&A, 556, A133
Saumon, D., & Marley, M. S. 2008, ApJ, 689, 1327
Schneider, A. C., Cushing, M. C., Kirkpatrick, J. D., et al. 2014, AJ, 147, 34
Schneider, A. C., Windsor, J., Cushing, M. C., Kirkpatrick, J. D., & Wright, E. L. 2016, ApJL, 822, L1
Schneider, A. C., Meisner, A. M., Gagne, J., et al. 2021, ApJ, 921, 140
Scholz, R. D. 2010, A&A, 510, L8
Spergel, D., Gehrels, N., Baltay, C., et al. 2015, arXiv:1503.03757
Strampelli, G. M., Aguilar, J., Pueyo, L., et al. 2020, ApJ, 896, 81
The Dark Energy Survey Collaboration 2005, astro. arXiv:astro-ph/0510346
Todorov, K. O., Luhman, K. L., Konopacky, Q. M., et al. 2014, ApJ, 788, 40
Vacca, W. D., Cushing, M. C., & Rayner, J. T. 2003, PASP, 115, 389
Vos, J. M., Allers, K. N., & Biller, B. A. 2017, ApJ, 842, 78
Ward-Duong, K., Patience, J., De Rosa, R. J., et al. 2015, MNRAS, 449, 2618
Wilson, J. C., Henderson, C. P., Herter, T. L., et al. 2004, Proc. SPIE, 5492, 1295
Winters, J. G., Henry, T. J., Jao, W.-C., et al. 2019, AJ, 157, 216
Wright, E. L., Eisenhardt, P. R. M., Mainzer, A. K., et al. 2010, AJ, 140, 1868
Zalesky, J. A., Line, M. R., Schneider, A. C., & Patience, J. 2019, ApJ, 877, 24
Zhang, Z. H., Galvez-Ortiz, M. C., Pinfield, D. J., et al. 2018, MNRAS, 480, 5447
Zuckerman, B., & Song, I. 2009, A&A, 493, 1149